

A Design of the Slow Extraction System in the JHF 50-GeV Proton Synchrotron

Noboru TOKUDA*, Masahito TOMIZAWA, Yoshitsugu ARAKAKI, Shinji MACHIDA,
Yosiharu MORI, Tamaki WATANABE

Accelerator Laboratory, High Energy Accelerator Research Organization

3-2-1 Midori-cho, Tanashi, Tokyo 188, JAPAN

*1-1 Oho, Tsukuba, Ibaraki 305, JAPAN

Abstract

A slow extraction system using the third-integer resonance technique has been designed for the 50-GeV main ring of the Japan Hadron Facility (JHF). The septa are an electrostatic septum (ESS) and five magnetic ones. The former and the latter are installed in different long straight sections, which are apart from each other by 1/2 circumference. Beam simulations show that the beam loss at the ESS wires is $\sim 1\%$.

1 Introduction

The JHF 50-GeV main ring has four long straight sections (LSS's), each of which is 60 m long, in the present lattice version [1]. An ordinary layout of an electrostatic septum (ESS) and magnetic septa would be such that all of them are installed in one LSS. This is, however, infeasible in our case. The beam energy is so high that the deflection angle in the ESS is small, and hence, at the entrance of the magnetic septum that follows the ESS, the separation between the extracted beam and the circulating one is not large enough. We therefore install the ESS in the LSS located in the opposite side of the LSS for the magnetic septa: the LSS's are apart from each other by 1/2 circumference.¹ In the present design, the length and field of the ESS (we call it preseptum) are respectively 1.5 m and 6.8 MV/m, yielding a deflection angle of 0.2 mrad. Despite of the small deflection, the beam-beam separation at the first magnetic septum is large enough to insert a 1-mm-thick septum. The beam passes through another four magnetic septa, and at the exit of the final septum, it is apart from the equilibrium orbit by 44 cm.

This paper describes the layout of the extraction devices and beam simulation results for an extraction scheme using the third-order resonance.

2 Layout of Devices and Orbits

The layout of the LSS for the preseptum is sketched in Fig. 1. The preseptum is placed at the exit of a focusing quadrupole magnet, because the β -function (β_x) is large there and the step size is large accordingly; this is advantageous to reduce the beam loss at the septum wires. The α -function (α_x) is also large. Owing to this, two of the three arms going out from the separatrix cross

¹The LSS between the above LSS's is used for the rf cavities.

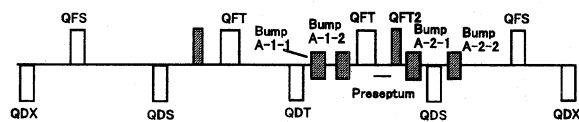


Figure 1: Layout of the preseptum and the bump magnets (A group).

the septum wire, and the particles in the two arms are extracted. For a remedy, we have installed two focusing quadrupole magnets (QFT2's) additionally only in this LSS. During the extraction period, this LSS is operated in a special manner (slow extraction mode): the QFT2 magnets are excited; and the field gradients of the lattice quadrupole magnets are different from those in the other LSS's. In the slow extraction mode, the LSS is matched to the adjacent arcs: the beam-optics functions are continuous at the LSS ends; the phase advance over the LSS is the same as that in the other LSS's ($\Delta\mu_x = 2\pi$, $\Delta\mu_y = \pi$). At the entrance of the preseptum the beam-optics functions are $\beta_x = 25$ m, $\alpha_x = 0.5$, $\eta_x = 0.35$ m.² The preseptum wires are positioned so that $(x, x') = (-43$ mm, -0.25 mrad) at the entrance end; the extracted beam is kicked inward. Four bump magnets (A group) produce an orbit with $(-15$ mm, 0 mrad) at the entrance of the preseptum.

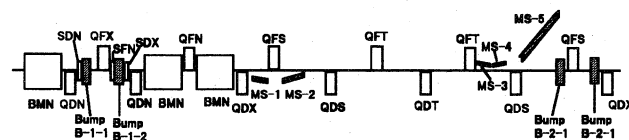


Figure 2: Layout of the magnetic septa (MS-1 through MS-5) and the bump magnets (B group).

The septa other than the preseptum are five magnetic ones (MS-1 ~ MS-5); their layout is shown in Fig. 2 along with bump magnets (B group). The phase advance between the preseptum and the first magnetic septum MS-1 is 3662° ; the extracted particles are kicked inward in MS-1 as well as in the preseptum. The particles receive further inward kick in MS-2 and outward kick in MS-3, -4, and -5. The bump orbit is such that $(x, x') = (-19.75$ mm, -2.11 mrad) at the entrance of the first magnetic

²In the normal operation, $\beta_x = 28$ m, $\alpha_x = 2.6$, $\eta_x = 0.29$ m.

3 Beam Simulation

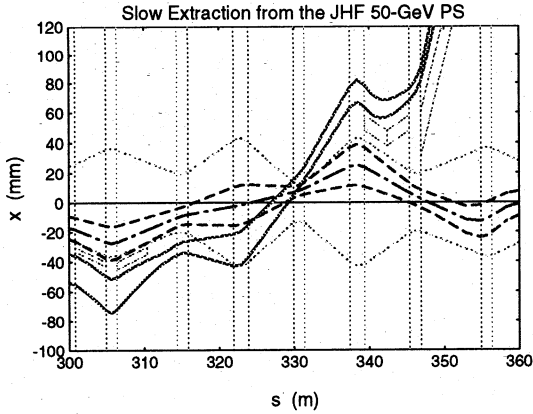


Figure 3: Beam envelopes in the long straight-section: 1) 3-GeV injected beam (dotted lines), 2) 50-GeV circulating beam (dashed lines), and 3) 50-GeV extracted beam (solid lines). The coils of the magnetic septa are indicated by squares, and the edges of the quadrupole magnets by vertical lines.

septum MS-1.

Figure 3 shows beam envelopes in the long straight section for MS-1 through MS-5. The envelopes plotted here are 1) 3-GeV injected beam ($\epsilon = 54 \pi \text{ mm} \cdot \text{mrad}$, $\Delta p/p = \pm 0.42\%$, COD = $\pm 1 \text{ mm}$), 2) 50-GeV circulating beam ($\epsilon = 6.1 \pi \text{ mm} \cdot \text{mrad}$), 3) 50-GeV extracted beam. The parameters of the septa are listed in Tables 1 and 2. At the exit of the final septum MS-5 the beam is separated so far from the equilibrium orbit that it will not hit the yoke of the quadrupole magnet: the half width of the yoke is 410 mm, and the particles distribute in the range of $x = 445 \sim 472 \text{ mm}$.

Table 1
Parameters of the preseptum.

location	LST3.2
deflection angle	-0.2 mrad
electric field	6.79 MV/m
gap (wire-anode)	25 mm
voltage	0.170 MV

Table 2
Parameters of magnetic septa.

septum manget	MS-1	MS-2	MS-3	MS-4	MS-5
location	LST1	LST2	LST3.2	LST3.2	LST2.2
θ_{kick} (mrad)	-1.8	-1.4	9.0	3.0	64.0
B (tesla)	0.133	0.068	0.665	0.222	1.673
length (m)	2.3	3.5	2.3	2.3	6.5
gap (mm)	40	40	40	40	40
NI (kA·turns)	0.423	2.16	21.2	7.05	53.2
t_{septum} (mm)	1	2	10	10	30
J_{septum} (A/mm ²)	106	27	53	18	44

For the design of the 50 GeV MR, a computer code has been developed. This code executes multi-particle tracking in a $x-x'-y-y'-\Delta p/p$ phase space using transfer matrices of the lowest order. A thin lens approximation is used for the sextupole and higher order fields. The initial beam distributions are assumed to be a uniform one in a four-dimensional ellipse (x, x', y, y') and a parabolic one for $\Delta p/p$.

The position of the preseptum wires is set to -43 mm. The horizontal and vertical emittances are $6.1\pi \text{ mm} \cdot \text{mrad}$, and the momentum spread is $\pm 0.23\%$. The horizontal betatron tune is approached to the resonance $65/3$ by ramping the lattice quadrupole magnets (QFNs). The horizontal and vertical chromaticity is set to zero by the sextupole magnets for the chromaticity correction.

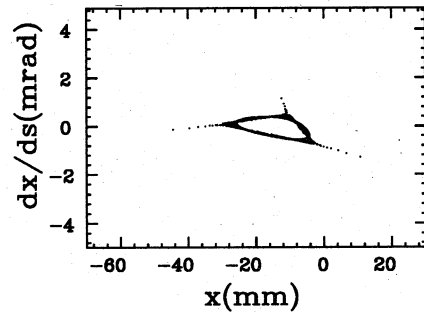


Figure 4: Phase space plot of a single particle at the entrance of the preseptum.

Figure 4 shows a phase space plot of a single particle by the simulation. In this case, the separatrix is rotated by 18° in the normalized phase space. As a result, the extracted particles have the negative x' for the bump orbit at the entrance of the preseptum, which is necessary to deliver the particles inward for the MS-1. The horizontal betatron tune is approached to the resonance of 21.666 from a higher value. The tune shift per one turn is 5.5×10^{-6} . The position and the angle of the bump orbit are -15 mm and 0 mrad at the preseptum. Figure 5 shows the phase space distribution and the profile of the extracted beam at the preseptum entrance. The loss at the wires depends on the beam density and the angular spread around the wires. The angular spread near the wires is about 0.7 mrad. When the preseptum length is 1.5 m and a thickness of the wires is 0.1 mm, the obtained minimum beam loss is 1.3%.

The beam loss is also caused by particles not extracted from the ring in the extraction process. These particles are remained in the ring and lost in the following deceleration process. This loss rate was investigated from the point of view of a tune ramping speed. Figure 6 shows the rate of remained particles as a function of the tune ramping speed. The remained rate becomes almost zero for slower speed than 1×10^{-6} per turn, which corresponds to the spill time of about 50 ms.

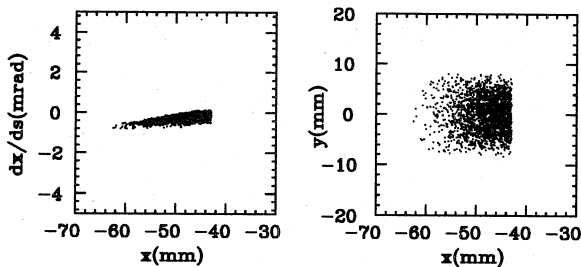


Figure 5: Phase space distribution and profile of the extracted beam at the preseptum entrance.

There are two kinds of particles' hit to the preseptum wires. One is the head-on hit: the entrance-end wire is hit. This loss depends on a particle density near the wires. To reduce it, the step size should be chosen to be as large as possible within the gap length of the preseptum. The other hit is such that particles hit the side of the wires. In this case, the loss depends on the angular spread of the particles near the wires as well as the particle density. In the present design, the preseptum is placed at the position with the small dispersion (0.35 m), and the chromaticity is set to zero. In this case, the angular spread is mainly caused by the emittance of the circulating beam, because the separatrix shrinks with the tune shift. This angular spread can be decreased by varying the angle of the bump orbit during the extraction. In the simulation, the angle of the bump orbit is varied from -0.8 mrad to 0.65 mrad to keep the position at -15 mm. Figure 7 shows the phase space distribution and the profile of the extracted beam at the preseptum entrance. The angular spread has been reduced by varying the bump orbit (cf. Fig. 5). As a result, the beam loss at the preseptum wires decreased to 0.9%. The emittance of the extracted beam integrated over the extraction period has decreased by a factor of about 3.

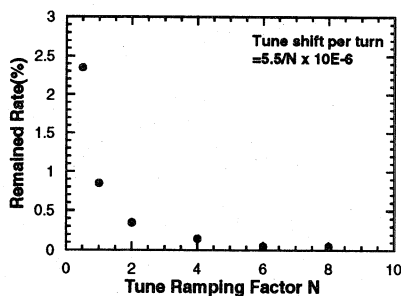


Figure 6: Rate of the remained particles as a function of the tune ramping speed.

4 Concluding Remarks

We have found a scheme of the extraction from the 50-GeV ring. The third-order resonance technique has been

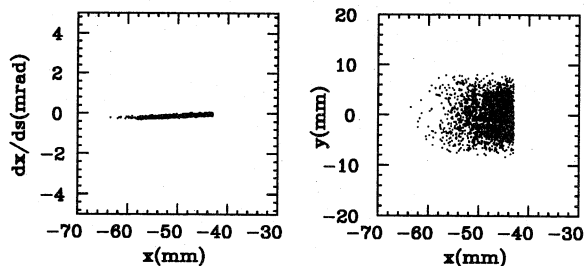


Figure 7: Phase space distribution and profile at the preseptum entrance. The bump orbit is varied during the extraction.

used in our design. The important issue is to minimize the beam loss. Simulations show that the beam loss at the preseptum wires is 1%. We will try to reduce the loss further, and improve the simulation for more precise estimation (the ripples of the magnetic fields have not been taken into account). From the point of view of clearing the beam from the ring, the half-integer resonance with non-zero stopband width is more advantageous. Studies on the beam loss using half-integer extraction will be done. The decision which resonance to adopt will be made after comparing the performances.

From the point of view of hardware, the bump and the septum magnets will be ordinary ones: their magnetic fields and current densities are not far different from those used now in the KEK 12-GeV proton synchrotron [2]. The preseptum needs R&D before fabrication. In the present design the required field strength is 6.8 MV/m. The voltage is 170 kV for a wire-anode gap of 25 mm. In order to attain such a high voltage, we are planning to construct an electrostatic septum (ESS) for tests. The main issues are the structure for the feed of high voltages (the goal is 200 kV) and the material of the wires and the anode. The length of the R&D ESS will be around 0.7 m, and the transverse cross section will be close to a real ESS. The start of the tests is scheduled for the next spring.

Acknowledgment

The authors thank S. Ohnuma for valuable suggestions and discussions.

References

- [1] Beam Optics and Dynamics Working Group, "Design of JHP Synchrotrons —Beam Optics and Beam Dynamics (in Japanese)", INS, JHP-30, July, 1996.
- [2] Y. Shoji *et al.*, "Slow Extraction System of the KEK-PS", KEK Report 93-10, 1993.